A novel centrosome-associated protein with affinity for microtubules

Pascal A. Stein[1], Christopher P. Toret[1], Adrian N. Salic[2], Melissa M. Rolls[1] and Tom A. Rapoport[1,*]

[1]Howard Hughes Medical Institute and Department of Cell Biology, and [2]Department of Cell Biology, Harvard Medical School, 240 Longwood Avenue, Boston, MA 02115-6091, USA

*Author for correspondence (e-mail: tom_rapoport@hms.harvard.edu)

Accepted 12 June 2002
Journal of Cell Science 115, 3389-3402 (2002) © The Company of Biologists Ltd

Summary

We have identified a novel mammalian protein, MIR1, with microtubule-binding activity. MIR1 is a relative of MID1/midin, the protein implicated in Opitz G/BBB syndrome. In tissue culture cells, MIR1 is enriched at the centrosome. MIR1 dissociates from centrosomes at the G2/M transition and is recruited back to spindle poles during anaphase. When overexpressed during interphase, MIR1 binds along microtubule filaments, which become stabilized, bundled and detached from the centrosome. In mitosis, overexpressed MIR1 dissociates from microtubules but still affects the normally focused localization of γ-tubulin in spindle poles. Tight binding to microtubules in interphase appears to require an oligomeric state of MIR1, and phosphorylation in mitosis at predicted cyclin-dependent kinase (cdk) sites weakens the interaction.

Key words: Microtubule, Centrosome, Phosphorylation, Cell cycle

Introduction

Microtubules are inherently polar filaments, polymerized in a head-to-tail fashion from dimers of α- and β-tubulin. As a result, the ends of the polymer are unequal, exhibiting different assembly and disassembly characteristics. The plus end of microtubules is very dynamic, undergoing alternating slow growth and rapid shrinking. The minus end is more stable (Desai and Mitchison, 1997). In many proliferating cells during the interphase of the cell cycle, the minus ends of most microtubules are anchored in the centrosome, and the plus ends extend to the cell periphery. This arrangement allows, for example, the Golgi apparatus to be concentrated near the nucleus by the minus-end-directed motor dynein (Lippincott-Schwartz, 1998). During mitosis, many of the interphase functions of microtubules are lost; instead, microtubules mainly serve as spindles to orient and segregate chromosomes. Microtubules become dramatically more dynamic, even at their minus ends, which are located at the spindle poles (Hyman and Karsenti, 1996; Shirasu et al., 1999).

In many cells, the centrosome serves as microtubule-organizing center. It is described morphologically by a central pair of centrioles surrounded by an electron-dense meshwork, the peri-centriolar material (PCM). Centrioles, a pair of structures of nine-fold symmetry composed of tubulin filaments, direct the replication of the centrosome and are required for the integrity of the PCM (Bobinnec et al., 1998). The PCM is composed of an insoluble fibrous network, the centromatrix, with which many proteins are associated, including those that promote microtubule nucleation and anchoring. The centrosome is a dynamic structure that is remodeled not only during replication in interphase but also at the onset of mitosis, as it acquires many new components involved in generating the spindle pole (for a review, see Stearns, 2001).

A large number of proteins interact with microtubules (microtubule-associated proteins or MAPs), and their function may be regulated by restricting their activity both spatially and temporally. Some proteins that modulate polymer dynamics, for example Op18/stathmin (Belmont and Mitchison, 1996), are only transiently associated with microtubules, whereas others, like MAP4 (Bulinski and Borisy, 1980), are stably associated with them. In addition, some bind only to the tips and others along the length of the polymer. Microtubule-associated proteins are also found localized to specific cellular sites, such as the centrosome. The γ-tubulin ring complex (γ-TuRC), which promotes microtubule nucleation (Zheng et al., 1995), and ninein, which acts to anchor prepolymerized microtubules (Mogensen et al., 2000), are localized at the minus ends of microtubules and are concentrated at the centrosome. Other proteins, such as katanin, although capable of binding along microtubule filaments, are nonetheless restricted to the centrosomal area (Hartman et al., 1998). The interaction of many MAPs with microtubules is regulated during the cell cycle; at some stages they may either have reduced or no affinity for microtubules (Andersen, 1998; Shirasu et al., 1999). A common mechanism modulating microtubule association is phosphorylation of the MAPs.

Many known microtubule-binding proteins were identified in co-pelleting or binding assays in vitro (Borisy et al., 1975; Kellogg et al., 1989). These methods allow easy manipulation of the experimental parameters and permit the isolation of defined classes of microtubule binding proteins, but the conditions of binding may not be the same as in the cell. One way to approach more physiological conditions is to use genetic screens. In systems in which genetic screens are difficult, visual methods in intact cells may be used to identify microtubule-binding proteins. We have previously described a new method in which proteins are identified on the basis of

their specific intracellular location (Rolls et al., 1999). Here we have used this procedure to identify a novel protein with microtubule-binding activity that displays a regulated association with the centrosome.

Materials and Methods

Cell culture, transfections and manipulations

BHK-21 [CCL-10, ATCC (American Type Culture Collection)], U2OS (HTB-96, ATCC) and COS cells (gifts from F. McKeon, Harvard Medical School) were grown in DME supplemented with 10% defined FBS (Hyclone Laboratories Inc.), 100 U/ml each penicillin and streptomycin and GLUTAMAX-1 (GIBCO BRL) in a humidified 37°C incubator with 5% CO_2. U373 cells were grown under the same conditions but using DME+HEP as the base medium. Cells were transfected with calcium phosphate as the carrier and processed about 20 hours after transfection. For immunofluorescence, cells were grown on 18 mm round coverslips and were transfected with 1 μg of DNA, otherwise they were grown in six-well dishes or 10 cm plates, and the amount of DNA used was scaled up accordingly. For co- and triple transfections, the maximum total amount of DNA used was 2 μg; when expression levels of a given construct were titrated, DNA amounts were kept constant by including appropriate amounts of non-expressing carrier DNA. To disrupt microtubules, cells were incubated at 4°C for 30 minutes and then treated with 3 μg/ml nocodazole for another 30 minutes. To stabilize microtubules, cells were treated with 4 μM taxol (gift from Drug Synthesis and Chemistry Branch, NCI) for 1 hour. To solubilize membrane compartments, cells first were briefly washed in BRB80 buffer (80 mM Pipes 6.8, 1 mM $MgCl_2$, 1 mM EGTA), and detergent treatment was performed with 0.1% or 1.0% Triton X-100 in BRB80 buffer supplemented with 4 mM EGTA and 2 μM taxol (to maintain microtubules) at 37°C for 4 minutes.

DNA manipulations of MIR1 coding sequence

Quadruple amino-acid substitutions were introduced into the MIR1 protein by mutating MIR1 DNA (clone VLP 27=GFP-MIR1) with a single continuous mutagenic oligonucleotide using the Gene Editor kit (Promega Corp) to produce GFP-MIR1A and GFP-MIR1DE. Full-length wild-type and mutant MIR1 coding sequences were transferred into a series of vectors, including pECFP-C3mn, pEYFP-C3mn (Rolls et al., 1999), pCS2-5myc (gift from M. Kirschner, Harvard Medical School), pcDNA3-HA (gift from F. McKeon, Harvard Medical School), pcDNA3, pET (Novagen, Madison, WI) and pFastBac-HTB (Gibco BRL, Carlsbad, CA) by PCR, using specific primers containing appropriate restriction sites and then subcloning the amplified DNA. The final constructs consisted of a tag, if present, an intervening linker encoding three glycines and the MIR1 coding sequence. Fragments of MIR1 coding sequence were obtained and treated similarly, resulting in the following truncated proteins: tN (aa1-297), tNP (aa1-332), tPC (aa298-496), tC (aa333-496), tP (aa270-350), delC-C (aa108-496) and tFn3 (aa108-332).

Northern analysis

The entire MIR1 coding sequence was ^{32}P-dCTP-labeled using Prime-It kit (Stratagene), purified by gel filtration and incubated on RNA blots [human Multiple Tissue Northern, MTN, and human RNA Master Blot (CLONTECH Laboratories, Inc.)] according to the manufacturer's instructions and using the manufacturer's reagents.

Production of antibodies and of recombinant MIR1 protein

Synthetic peptide 27.2 [CLQKRGSATSS (Biopolymers Laboratory)] encompassing amino acids 480-490 near the C-terminus was coupled to three different carrier proteins, keyhole limpet hemocyanin (Calbiochem-Novabiochem, San Diego, CA), BSA (Calbiochem-Novabiochem) and ovalbumin (Pierce Chemical, Rockford, IL). A rabbit was immunized with each of these peptide conjugates administered in succession (Cocalico, Reamstown, PA), yielding antiserum Ab284. Antiserum Ab284 was affinity-purified over a Sulfo-Link (Pierce Chemical) column to which peptide 27.2 had been coupled and concentrated over a hydroxyapatite (Bio-Rad Laboratories, Hercules, CA) column.

To generate Ab520, the MIR1 was produced as inclusion bodies by bacterial expression in *E. coli*. Briefly, the pellet of *E. coli* induced to express MIR1 was rinsed in PBS and resuspended in 40 ml of lysis buffer (PBS supplemented with protease inhibitors), and the cells were disrupted using a French press. The lysate was centrifuged at 3000 ***g*** for 10 minutes, the supernatant recovered and centrifuged again at 28,000 ***g*** for 20 minutes. This pellet was treated with PBS, 1% Tween 20 and centrifuged as before. An aliquot of the pellet resuspended in PBS was used to immunize a rabbit, yielding Ab520. Ab520 was affinity purified by absorption of the serum to, and low pH elution from, a strip of nitrocellulose-containing immobilized MIR1.

Recombinant His-tagged MIR1 protein was produced in a baculovirus expression system and purified by virtue of the interaction of the 6×His tag with Ni-NTA resin (Qiagen, Valencia, CA). Briefly, the pellet from 200 ml of infected Sf9 insect cells was resuspended in 25 ml of lysis buffer (20 mM Hepes pH 7.5, 300 mM NaCl, 1% Tween 20, 10 mM imidazole), supplemented with protease inhibitor and sonicated. Cell debris was removed by centrifugation at 30,000 ***g*** for 20 minutes; lysate was bound in batch to 1 ml Ni-NTA agarose beads and incubated for 90 minutes. Ni-NTA beads were collected and washed, once in lysis buffer and then sequentially in wash buffers W1-W3 (20 mM Hepes pH 7.5, 10 mM imidazole, with additionally, for W1, 400 mM NaCl, 1% Tween 20; for W2, 50 mM NaCl, 1% Tween 20; and for W3, 50 mM NaCl). Recombinant His-MIR1 was eluted in 10 ml elution buffer EB (20 mM Hepes 8.0, 250 mM imidazole), dialyzed and frozen in aliquots at –80°C. Although the majority of MIR1 was lost as aggregates with the cell pellet, 1% remained soluble throughout the procedure but was prone to precipitation upon concentration. Thus it was kept at 100 μg/ml.

Immunoblots

Roughly equal aliquots of the postnuclear lysate fraction derived from rat liver or brain, cow brain, U2OS cells, untransfected or MIR1-transfected BHK-21 cells were used for immunoblots with affinity-purified Ab284. Proteins were separated by SDS-PAGE and transferred to nitrocellulose. The blot was probed with Ab284 at 1:2000 dilution, and proteins were detected by chemiluminescence.

Microtubule co-sedimentation assay

^{35}S-labelled MIR1 protein was synthesized in a reticulocyte lysate using TNT kit (Promega, Madison, WI). Microtubules were polymerized from purified tubulin (Cytoskeleton, Boulder, CO) to a final concentration of 5 mg/ml in BRB80 buffer supplemented with 1 mM GTP and protease inhibitor cocktail and were then taxol-stabilized according to the protocol on the Mitchison laboratory webpage (http://iccbweb.med.harvard.edu/ mitchisonlab/Pages). An aliquot of MIR1 protein in reticulocyte lysate was diluted into BRB80 buffer supplemented with 5 μM taxol and protease inhibitor cocktail, and aggregates were spun out at 20,000 ***g*** for 20 minutes at 4°C. Samples were warmed to 30°C, one tenth of the volume of polymerized microtubule stock was added, and then incubated for 15 minutes. Samples were spun through a 40% sucrose cushion for 7 minutes at 200,000 ***g*** in a TLA-100 rotor (Beckman) at 22°C; pellets were washed and resuspended in SDS-PAGE sample buffer. Proteins

were separated by SDS-PAGE and visualized by autoradiography. Controls were treated identically, except that one tenth of the volume of BRB80 buffer instead of microtubules was added to the sample. The experiment was performed in triplicate.

Sucrose density gradients

9%-15% sucrose gradients were set up in 41 mm centrifuge tubes of 5 mm diameter in a buffer containing 20 mM Hepes pH 7.4, 50 mM NaCl, 1 mM $MgCl_2$, 2 mM DTT supplemented with protease inhibitor cocktail, for a total volume of 560 μl. 100 μl of precleared purified MIR1 protein, obtained from a baculovirus expression system, were layered on top of the gradient and the samples were centrifuged for 4 hours at 33,000 ***g*** in a swinging bucket SW55 rotor (Beckman). After centrifugation, 30 μl fractions were resuspended in an equal volume of sample buffer and separated by 7%-15% SDS-PAGE. Reference standards were BSA (66 kDa), aldolase (150 kDa) and catalase (256 kDa).

Immunofluorescence staining

Cells on 18 mm coverslips were routinely fixed in –20°C methanol for 5 minutes and rehydrated in PBS+ or, to better preserve membrane-bound organelles, fixed in 3% paraformaldehyde/PBS+ for 15 minutes at room temperature and then quenched with 10 mM glycine/PBS+. Fixed cells were blocked in PBS/10% calf serum/0.1% Triton X-100/0.5 mM NaN_3 and subsequently incubated for 90 minutes to overnight in primary antibody diluted into PBS/2% calf serum/0.1% Triton X-100/0.5 mM NaN_3. Cells were washed repeatedly in PBS/0.1% Triton X-100 and incubated for 45 minutes with a secondary antibody diluted 1:500 in same antibody buffer. Nuclei were stained with 0.2 μM Hoechst 33258 for 2 minutes and cells washed in PBS.

Ab284 was preadsorbed with 50-fold excess MIR1 protein in antibody dilution buffer for 2 hours, and complexes were removed by centrifugation in a tabletop centrifuge at 20,000 ***g*** for 10 minutes. The supernatant was used as a control for specificity of antigen recognition by Ab284.

Antibodies were used at the following dilutions: Ab284 (MIR1) at 1:1,000; Ab520 (MIR1) at 1:750; M1α (α-tubulin, Sigma) at 1:10,000; mAb GTU-88 (γ-tubulin, Sigma) at 1:2,000; mAb 6-11B-1 (acetylated tubulin, Sigma) at 1:2,000; human autoimmune serum 5051 (centrosomal antigens, gift from M. Kirschner, Harvard Medical School) at 1:1,000; α-centrin (gift from M. Bornens, Institut Curie) at 1:1,000; GM130 (Golgi peripheral protein) at 1:1,000; α-NUP62 (nuclear pore marker) at 1:1,000; mAb v9 (vimentin, Sigma) at 1:1,000; and secondary antibodies rhodamine α-mouse, rhodamine α-rabbit (Jackson Labs, Bar Harbor, ME), AlexaFluor488 α-mouse (Molecular Probes, Eugene, OR) at 1:500.

Fluorescence microscopy and imaging

Coverslips were mounted in 90% glycerol/10% Tris pH 7.5. For routine observations, samples were viewed on an Axioplan II microscope with 63× or 100× Apochromat objectives (Zeiss, Thornwood, NJ) fitted with a Hamamatsu 4742-95 12-bit cooled CCD camera (Hamamatsu Photonics, Bridgewater, NJ). Fluorescence was viewed with appropriate narrow band pass filter sets (Chroma Technology, Brattleboro, VT). When samples were imaged for YFP and rhodamine-labelled structures, a Texas Red filter set was used for the rhodamine signal to achieve better channel separation. Image-Pro Plus 3.0 (Media Cybernetics, configured by Phase 3 Imaging Sytems) or Openlabs (Improvision, Lexington, MA) software was used for image capture and processing. In some experiments, cells were viewed on a DeltaVision system (Applied Precision Instruments, Issaquah, WA) in which case optical sections were taken in 0.2 μm intervals and images were deconvoluted by applying an iterative deconvolution algorithm. In the final images, a stack of image sections recorded at different wavelengths was collapsed into a projection view and the individual images overlayed.

Results

Isolation of MIR1

In our visual screen, pools of cDNAs from an osteosarcoma cell line (USO2) were expressed in BHK cells as proteins fused to N-terminal green fluorescent protein (GFP). When a specific and recognizable fluorescent pattern was seen, the cDNA pool was split and subpools re-tested until the cDNA clone responsible for the pattern was identified. The procedure allowed the isolation of markers for different cell structures and resulted in the identification of a novel nuclear envelope protein, called nurim (Rolls et al., 1999). Using the same approach, we isolated clone VLP27 that exhibited a striking filamentous pattern. The fluorescence pattern of the GFP fusion protein (Fig. 1A, first panel) coincided with the staining of microtubules as revealed by immunofluorescence with the monoclonal tubulin antibody M1α (Fig. 1A, second panel). In cells expressing VLP27 at high levels, the normal interphase pattern of microtubules was severely perturbed; a whorl of microtubules was seen around the nucleus, and the microtubules were often bundled. This altered microtubule pattern was reminiscent of that produced by the overexpression of other microtubule-associated proteins (MAPs), such as tau or MAP2 (Lewis et al., 1989), and suggested that clone VLP27 codes for a microtubule-binding protein. At very low levels of VLP27 expression, the fluorescence pattern tracked along single microtubule filaments (Fig. 1A, third and fourth panel).

Sequencing of the clone VLP27 indicated that it encodes an unknown protein of 496 amino acids (accession number BAB13885). A BLAST search showed that it is related to MID1/midin and MID2/FXY2 (Fig. 1B) (Buchner et al., 1999; Perry et al., 1999; Quaderi et al., 1997; Schweiger et al., 1999). MID1/midin is reported to be associated with Opitz G/BBB syndrome, a disease in which ventral midline development is affected in areas such as the corpus callosum, lip and palate, heart, stomach and the intestinal and urogenital tract, presumably a result of closure defects. We called the new member of the protein family MIR1, for Mid Related Protein 1. Like MID1/midin, MIR1 contains a coiled-coil region (37% amino acid identity), followed by a Fn3 class fibronectin domain (53% identity) and finally a C-terminal B30.2 box (52% identity) (Fig. 1B). These regions are all thought to be protein-protein interaction domains. In MID1/midin, the B30.2 box acts as a microtubule interaction domain (Cainarca et al., 1999; Schweiger et al., 1999), but this domain is also found in other proteins that do not interact with microtubules (Henry et al., 1998). Interaction with microtubules may be essential for the biological function of MID1 because most mutations, other than null mutations, that cause Opitz syndrome map to this region (Cox et al., 2000; Quaderi et al., 1997; Schweiger et al., 1999). Notably absent from MIR1 are the N-terminal RING finger and double B-box domains, setting it apart from the RBCC class of proteins (the tripartite motif RING-finger–B-box–coiled-coil) to which MID1/midin belongs. A further unique feature of MIR1 is a 20 amino-acid region between the Fn3 and B30.2 domains, which contains multiple consensus sequences for proline-directed cyclin-dependent serine/

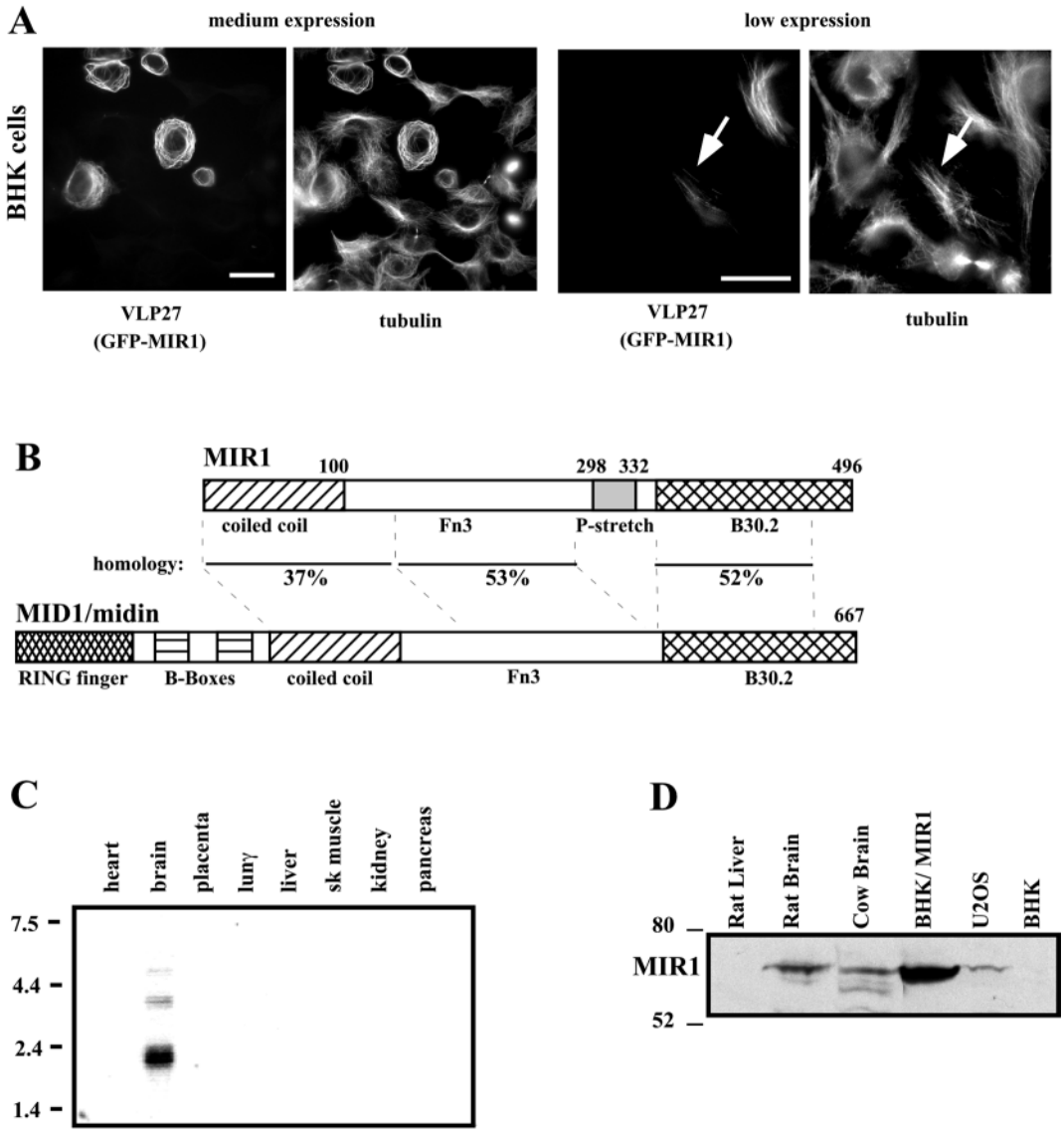

Fig. 1. Clone VLP27 encodes a novel microtubule-binding protein, MIR1. (A) The clone VLP27 (GFP-MIR1) was expressed at medium or low levels in BHK cells (first and third panel). The same cells were also stained with the tubulin antibody M1α (second and fourth panel). The magnification was 63× for the left two panels and 100× for the right ones. The arrows point to MIR1 staining of individual microtubules. (B) The diagram of the homology between MIR1 and its closest relative MID1/midin. The domain configuration is identical, except for the added P-stretch region and the missing N-terminal RING finger and B-Boxes in MIR1. (C) Northern blot of various human tissues probed against MIR1 RNA. (D) Immunoblot analysis of post-nuclear lysates from selected cells using the affinity-purified antibody Ab284 directed against MIR1. Lysate from BHK cells expressing untagged MIR1 was analyzed in parallel.

threonine kinases [cdks (Westendorf et al., 1994)], which we term the P-stretch (Fig. 6A).

Sequence searches did not reveal homologs in *Saccharomyces cerevisiae*, *Caenorhabditis elegans* or *Drosophila melanogaster*, in agreement with previous reports that B30.2 boxes are only found in vertebrates. In a northern blot analysis of multiple human tissues, MIR1 mRNA was found at particularly high levels in the brain (Fig. 1C). However, a detailed analysis with a more sensitive and comprehensive RNA dot blot also indicated significant expression in both fetal and adult thymus, the pituitary and in the testis (data not shown). Interestingly, whereas MIR1 mRNA was expressed in all areas of the adult brain, little of it was found in fetal brain. Many additional tissues revealed very low levels of MIR1 mRNA, whereas none was detected in cardiac or skeletal muscle (data not shown).

To ascertain whether the isolated clone contained the entire coding region of MIR1, we compared the size of an untagged version of MIR1 with that of the endogenous protein. An antibody was raised against a peptide contained in the C-terminus of MIR1 and affinity purified (Ab284). The antibody was used to probe lysates prepared from BHK cells overexpressing untagged MIR1. A major band of approximately 65 kDa was seen and was somewhat larger than predicted for the protein. It corresponded in size to the proteins detected in samples from U2OS cells and from brain cytosol (Fig. 1D). No immunoreactive protein was detected in liver cytosol or in non-transfected BHK cells, in agreement with the low expression of the mRNA seen in northern blot analysis. Further evidence that the clone comprised the entire coding sequence was provided by intron-exon analysis of the corresponding genomic sequence deposited in the htgs database by the Human Genome Project (accession number AC008616). The gene is located on the tip of the short arm of chromosome 19, and analysis of this chromosomal region using FGENES program returned the exact same open reading frame (data not shown).

Association of endogenous MIR1 with centrosomes is dependent on the stage of the cell cycle

We investigated the localization of endogenous MIR1 by

indirect immunofluorescence microscopy. First, to verify that the affinity-purified Ab284 antibody recognized MIR1 in intact cells, BHK cells overexpressing GFP-MIR1 were analyzed by both immunofluorescence and GFP fluorescence (Fig. 2A). The patterns showed a perfect overlap (left panels). In addition, when Ab284 was preincubated with MIR1 protein purified from a baculovirus expression system, specific staining was abolished (Fig. 2A, right panels).

Using this antibody, the most prominent localization of the endogenous protein was a bright spot peripheral to the nucleus (Fig. 2B, upper right panel and Fig. 2C), although a weaker, general punctate staining was also seen in the cytoplasm. At higher magnification, endogenous MIR1 was often seen in several spots clustered around the centrosome, revealed here by a marker for acetylated tubulin (Fig. 2B, left panel). The specificity of MIR1 staining was supported by the fact that the peri-centrosomal staining was no longer observed when the antibodies were preincubated with purified MIR1 protein (Fig. 2B, lower right panel). The peri-centrosomal staining of the endogenous protein was clearly distinct from the filamentous pattern seen with the overexpressed fusion protein GFP-MIR1 (see Fig. 2A). Localization of MIR1 at the centrosome was also found in COS cells and in the astrocytoma cell line U373 (Fig. 2C), and in neuronal cell lines, such as mouse CAD cells and human SH-SY5Y cells (data not shown). Staining at the centrosome was very weak in cell lines in which MIR1 mRNA expression is low, including BHK, Vero (not shown) and COS cells (Fig. 2C). There were small differences between different cell types with respect to the number of spots and the degree of their focus around the centrosome; γ-tubulin, a marker for centrosomes, did not show such variability in staining (Fig. 2C). MIR1 staining persisted at the centrosome after cells were treated with the microtubule-depolymerizing drug nocodazole (Fig. 2D). This observation suggests that MIR1 does not require an active microtubule-dependent mechanism to be maintained at the centrosome. We also raised a different antibody to the entire MIR1 protein purified from inclusion bodies after expression in *E. coli* (Ab520). When U373 cells were treated with this antibody, staining at the centrosomes was apparent, as well as a general cytoplasmic staining, supporting the observations made with Ab284 (Fig. 2F, left panels). However in addition, staining was occasionally observed as discrete punctae along single microtubules (right panels). Also, some labeling of perinuclear structures reminiscent of the Golgi apparatus was seen (data not shown).

MIR1 showed a cell-cycle-dependent association with the centrosome. When U373 cells were analyzed, MIR1 staining at the centrosome (marked with the autoimmune serum 5051) was seen during interphase, including during G2 phase when the centrosomes have duplicated (Fig. 2G). At prophase, MIR1 largely dissociated from the centrosomal region, and at metaphase it was distributed throughout the cell. MIR1 began to reappear at the spindle poles in late anaphase, and at telophase was mostly found at the spindle poles and in the midbody region (Fig. 2G; see also magnified view in Fig. 2F). The cell-cycle-stage-dependent profile of the staining pattern is further evidence of the specificity of the peri-centrosomal localization of MIR1. Interestingly, MIR1 behaves in an opposite manner to many centrosomal components identified to date, such as γ-tubulin or pericentrin (Dictenberg et al., 1998), which are enriched at the spindle poles during mitosis (Fig. 2G).

Overexpresssed MIR1 binds to and stabilizes microtubules

To begin to understand the localization of MIR1 with respect to the cell cycle stage, we analyzed overexpressed GFP-fusion constructs in BHK cells. Even at the lowest level of expression, GFP-MIR1 co-aligned with single microtubule filaments and did not localize to the centrosomes (Fig. 1A). Expression of untagged MIR1 produced the same pattern (data not shown). Similar results were also seen in U2OS cells and U373 cells, two cell lines in which MIR1 is seen associated with the centrosome endogenously. The lack of staining at the centrosome suggests that another protein present in limiting amounts may normally mediate the localization of MIR1.

Because even highly overexpressed GFP-MIR1 protein was predominantly seen in filamentous structures, the association of MIR1 with microtubules is likely to be direct. Microtubule binding and bundling was evident in all cell lines tested including *Xenopus* XTC cells (data not shown), indicating that the interaction is conserved between species. GFP-MIR1 did not colocalize with actin or vimentin fibers in GFP-MIR1-expressing cells that were stained with rhodamine-phalloidin or v9 antibodies (data not shown). Although GFP-MIR1 overexpression affected microtubules, the appearance of the endoplasmic reticulum, including the nuclear envelope, was not noticeably altered. By contrast, the Golgi apparatus, whose peri-nuclear location depends on a microtubule array emanating from the centrosome (Quintyne et al., 1999), was found to be dispersed in cells in which microtubules were bundled (data not shown).

To confirm MIR1 localization to microtubules, we treated BHK cells expressing GFP-MIR1 with nocodazole to disassemble the microtubule network. We then removed the drug and watched GFP-MIR1 during microtubule regrowth. Nocodazole was only able to disrupt microtubule networks at low or moderate levels of GFP-MIR1 expression; at high levels the microtubules became resistant to drug treatment (see below). When cells with a moderate expression level were observed after drug washout, GFP-MIR1 protein appeared on the microtubule asters as soon as they emerged from the centrosome (Fig. 3).

Since microtubules were resistant to nocodazole treatment in cells that highly express GFP-MIR1, we investigated the effect of MIR1 overexpression on microtubule stability. Modification of tubulin subunits by acetylation marks older microtubules and therefore indicates those that are more stable (Bulinski et al., 1988; Schulze et al., 1987). These microtubules can be detected with a specific antibody to acetylated tubulin. BHK cells, which like most fibroblast lines exhibit a half-life for microtubule turnover of the order of 10 minutes, contain very few acetylated microtubules (Fig. 4). By contrast, microtubules in all MIR1-expressing BHK cells showed increased acetylation, and these colocalized with MIR1 (Fig. 4). Therefore, MIR1 overexpression appears to affect microtubule stability.

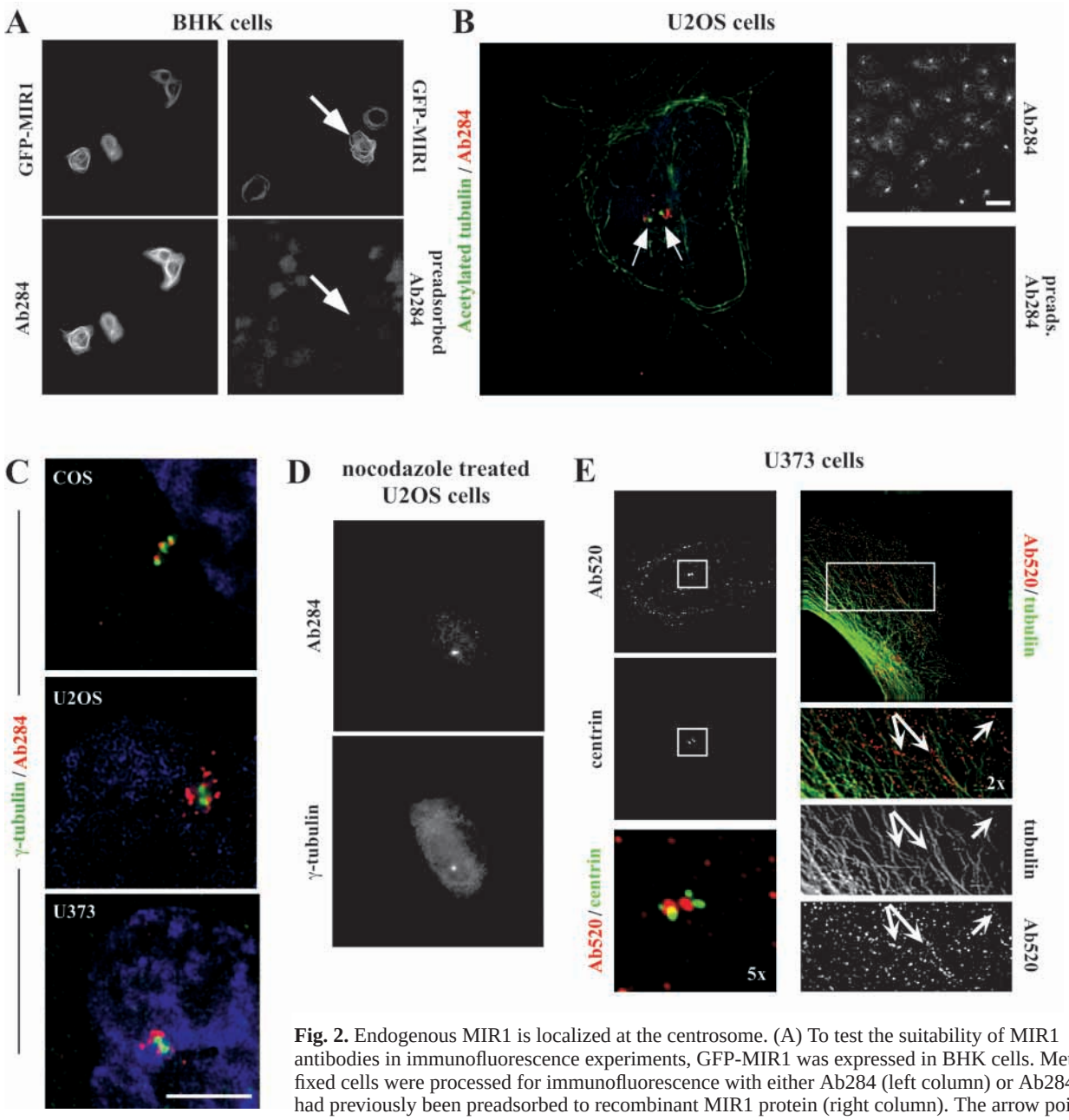

Fig. 2. Endogenous MIR1 is localized at the centrosome. (A) To test the suitability of MIR1 antibodies in immunofluorescence experiments, GFP-MIR1 was expressed in BHK cells. Methanol-fixed cells were processed for immunofluorescence with either Ab284 (left column) or Ab284 that had previously been preadsorbed to recombinant MIR1 protein (right column). The arrow points to a cell that shows GFP fluorescence but no staining with the pre-saturated antibody. Exposure times and image processing parameters were kept constant for all four panels to allow direct comparison (63× field). (B) Endogenous MIR1 in U2OS cells was visualized after fixation with methanol by immunofluorescence microscopy using Ab284. A low magnification view (upper right panel) shows prominent staining in the perinuclear region. A control shows staining with Ab284 that had previously been preadsorbed to recombinant MIR1 protein (lower right panel) (40× field). Bar 10 μm. A higher magnification picture is shown to the left. Co-staining with an antibody to acetylated tubulin reveals the location of the centrosome (arrows) (100× field). (C) MIR1 staining in different cell types was analyzed after fixation in methanol by immunofluorescence with Ab284 (rhodamine-conjugated secondary antibody). The cells were also stained with mAb GTU-88 to γ-tubulin (AlexaFluor-488-conjugated secondary antibody). Images, which were acquired at 100× on a Deltavision system, present a collapsed view of multiple processed sections. Bar, 5 μm. (D) MIR1 localization in U2OS cells persists at the centrosome in the absence of a microtubule network. MIR1 was stained with Ab284 and γ-tubulin with mAb GTU-88. (E) MIR1 localization with Ab520. Fixed U373 cells were stained for MIR1 with Ab520 and for centrosomes with an α-centrin antibody (left panels). Samples stained with M1α and Ab520 reveal MIR1 localized along individual microtubules as distinct spots (arrows in right panels, enlarged view). Images, acquired at 100× on a Deltavision system, are of a particular Z-section and have been processed by with an iterative deconvolution algorithm. (F) MIR1 localization in U373 cells during different stages of the cell cycle. Fixed cells were stained for MIR1 with Ab284 and for centrosomal antigens with human autoimmune serum 5051. The cells were also stained for DNA with Hoechst dye 33258. The arrow shows a cell going through the cell cycle. The arrowhead in the last panel shows another cell loss of MIR1 localization at the spindle poles in metaphase (100× field). (G) A higher magnification view of U373 cells in telophase. Staining was performed with Ab284 for MIR1 and with mAb GTU-88 for γ- tubulin. DNA was stained with Hoechst dye 33258. A Deltavision image was analyzed as in Fig. 1C. MIR1 staining is present at the centrosomes (arrows) and at the midbody (arrowhead) (100× field).

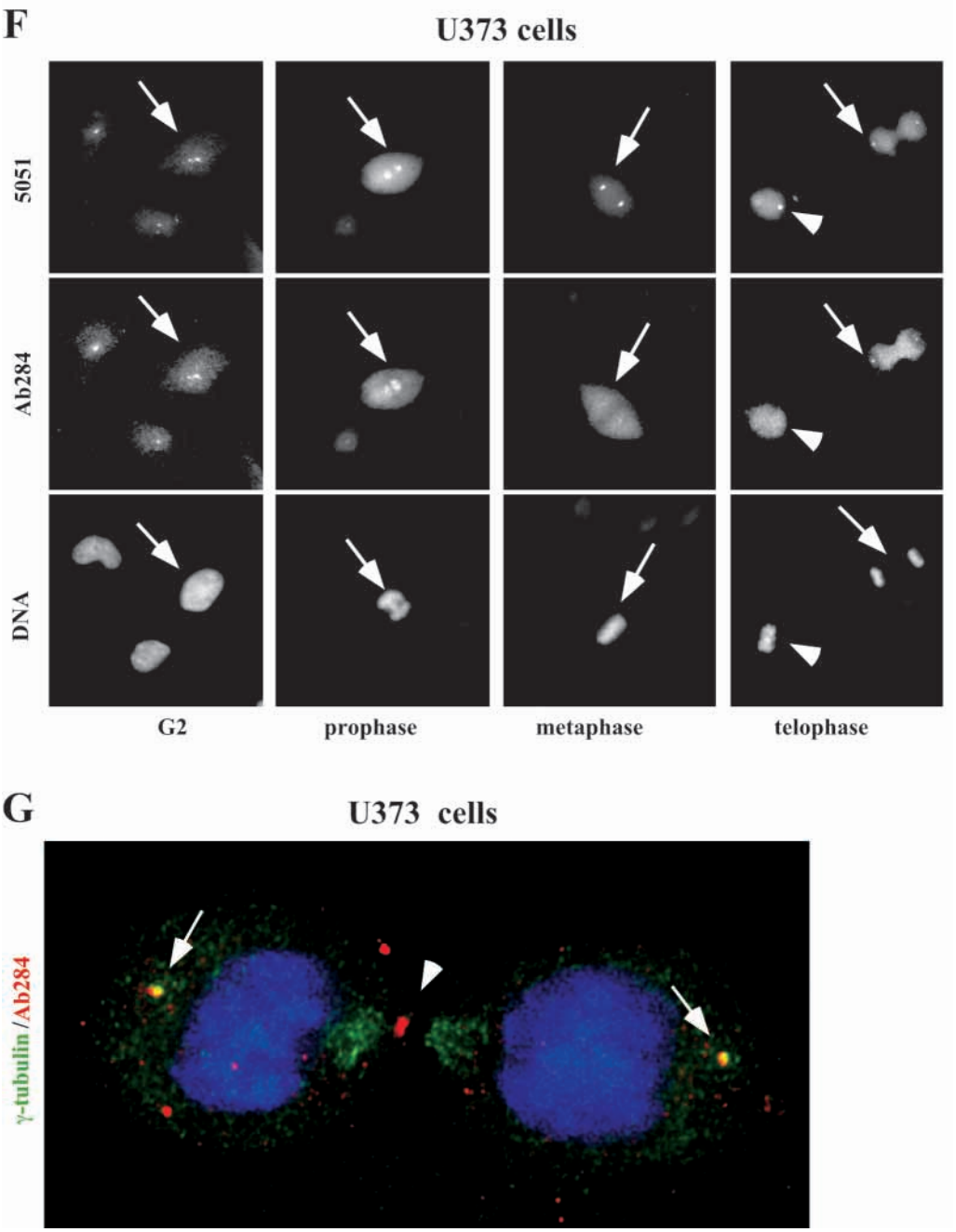

Regulated binding of MIR1 to microtubules

The association of GFP-MIR1 with microtubules was found to be dependent on the cell cycle stage. In BHK cells expressing GFP-MIR1 at a low or moderate level, the whorl-like appearance of MIR1 on microtubules seen in interphase (Fig. 5, left panels) disappeared at G2/M transition. At metaphase, most GFP-MIR1 was no longer associated with microtubules and was distributed diffusely, although a small amount remained on the spindle microtubules (Fig. 5, middle panel). At telophase, GFP-MIR1 reassociated with the wide band of interzone microtubules between dividing cells, as well as with the young microtubule asters (Fig. 5, right panel). Thus, like the localization of endogenous MIR1 at centrosomes, the association of overexpressed MIR1 with microtubules is cell-cycle-dependent.

Since overexpressed MIR1 showed regulation by the cell cycle, we considered the possibility that its direct phosphorylation by a cell-cycle-dependent kinase (cdk) may change its affinity for microtubules. The P-stretch of MIR1 contains four consensus cdk phosphorylation sites (Fig. 6A). To test the role of the P-stretch, we created two mutants. In MIR1A all four SP and TP sites were changed to AP to prevent phosphorylation at these sites; in MIR1DE these sites were changed to DP or EP to mimic the phosphorylated state.

When GFP-MIR1A was expressed in BHK cells, its expression pattern was indistinguishable from the wild-type protein during interphase (Fig. 6B, left panel), but in mitosis GFP-MIR1A remained associated with microtubules (right panel, arrow). Conversely, GFP-MIR1DE showed a markedly

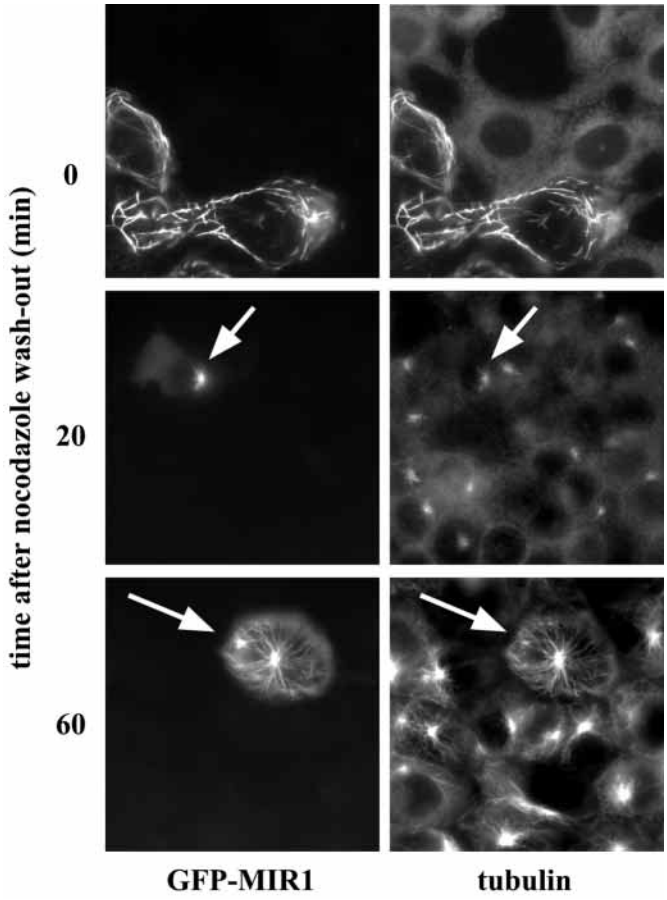

Fig. 3. Overexpressed MIR1 localizes to newly polymerized microtubules. BHK cells transfected with GFP-MIR1 were treated with nocadozole to depolymerize the microtubules. The drug was washed out and the microtubules allowed to repolymerize for the indicated times. The cells were fixed and analyzed for MIR1 by GFP fluorescence (left column) and for tubulin using the M1α antibody (right column). Arrows highlight transfected cells with newly formed microtubules.

reduced ability to associate with microtubules, even in interphase cells. In most cells, GFP fluorescence remained diffuse, and concentric microtubule swirls were seen only at high expression levels (Fig. 6C). Together, these results suggest that overexpressed MIR1 loses its affinity for microtubules during mitosis by phosphorylation in the P-stretch.

Since MIR1 is expressed in neuronal cells, which do not divide, we asked whether the protein can be regulated by the kinase cdk5, a cdk family member active in post-mitotic neurons (Hellmich et al., 1992; Meyerson et al., 1992; Tsai et al., 1993). In BHK cells that were triply transfected with GFP-MIR1, cdk5 and p35 [an activator of the kinase (Tsai et al., 1994)], GFP-MIR1 was no longer associated with microtubules, and the microtubule network appeared normal (Fig. 7, left panels). Thus, it seems that GFP-MIR1 can indeed be phosphorylated by cdk5/p35 and prevented from associating with microtubules. Controls supported this conclusion. A dominant-negative version of cdk5, cdk5DN, which lacks kinase activity (Nikolic et al., 1996), did not prevent the association of GFP-MIR1 with microtubules (middle panel). In addition, the non-phosphorylatable mutant GFP-MIR1A remained associated with microtubules even when cdk5 and p35 were present (right panel). These results support the idea that phosphorylation of the P-stretch of MIR1 can regulate microtubule association.

Effects of MIR1 overexpression on mitosis

Overexpression of wild-type MIR1 at moderate levels did not obviously affect the cell cycle, but at high levels it led to cell death (data not shown). Effects on the spindle pole morphology were frequently seen. γ-tubulin staining was often splayed out from the poles (Fig. 8A, compare the upper panel with the middle one). It is possible that overexpressed MIR1 competes for a factor that normally is involved in maintaining γ-tubulin at the spindle pole.

While overexpression of MIR1DE had no apparent effects on mitosis or spindle poles, expression of MIR1A resulted in a severely disorganized spindle where microtubule bundles criss-cross condensed chromosomes (Fig. 8A, lower panel). Since this could be caused by interference with the normally highly dynamic nature of these spindle microtubules, we examined whether the appearance of an abnormal mitotic spindle correlated with an increase in acetylated microtubules. Whereas the spindle in untransfected BHK cells or cells expressing low or medium levels of wild-type GFP-MIR1 did not contain detectable acetylated spindle microtubules (Fig. 8C, arrow head; Fig. 8B), the disorganized mitotic spindle decorated with GFP-MIR1A protein was strongly acetylated (Fig. 8C, arrow). Overexpression of GFP-MIR1A also had pronounced effects on the spindle poles. Multiple prominent spots of γ-tubulin were found dispersed along the disorganized spindle (Fig. 8A, lowest panel). Similar results were obtained when spindle poles were followed with the human autoimmune serum 5051 (data not shown). Moreover, later mitotic stages or cells undergoing cytokinesis were not observed,

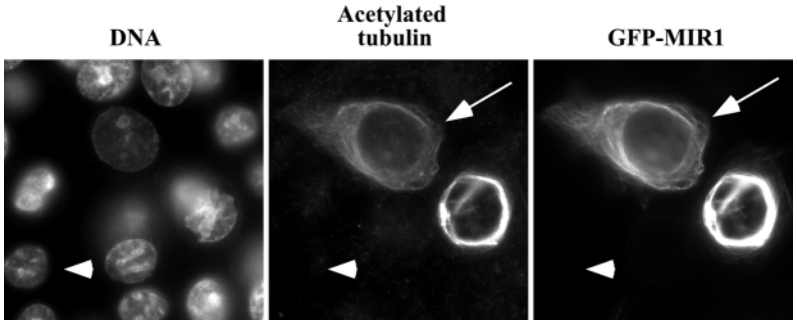

Fig. 4. Microtubules are long-lived in interphase cells overexpressing MIR1. BHK cells, overexpressing GFP-MIR1, were analyzed both by GFP fluorescence and by immunofluorescence with antibody 6-11B-1, which recognizes acetylated tubulin. The arrow indicates a transfected cell containing long-lived, acetylated microtubules. The arrowhead points to an untransfected cell.

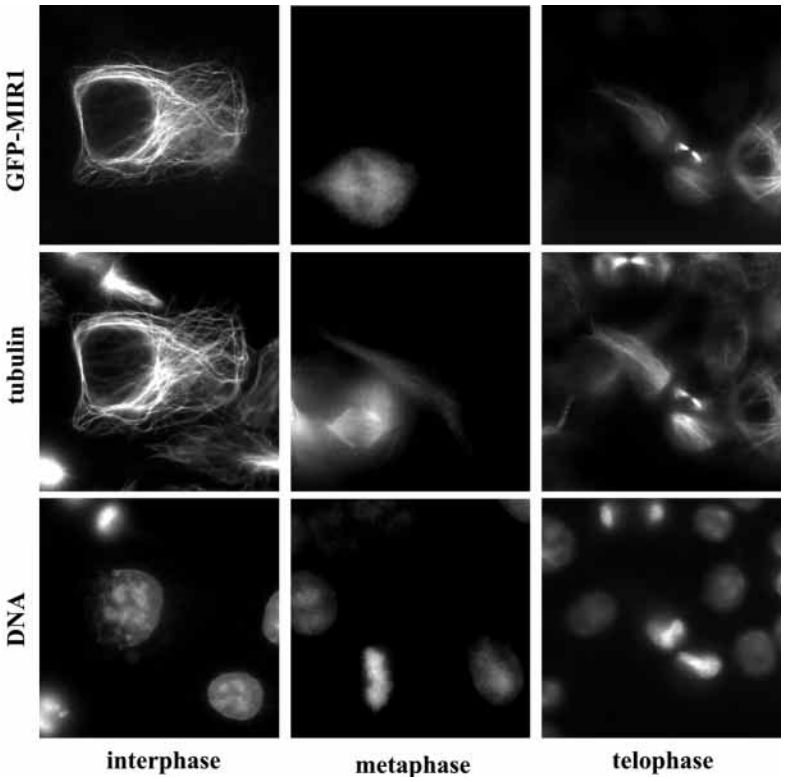

Fig. 5. The association of overexpressed MIR1 with microtubules is dependent on the cell cycle stage. BHK cells expressing GFP-MIR1 were analyzed at different stages of the cell cycle by GFP fluorescence and by staining with tubulin antibody M1α. The cells were also stained for DNA with Hoechst dye 33258.

indicating that cells overexpressing GFP-MIR1A were incapable of completing mitosis. A cell cycle arrest was also seen when untagged MIR1A mRNA was injected into one blastomere of a four-cell *Xenopus* embryo. By stage nine, a cluster of large cells that had stopped dividing was clearly evident (data not shown). Taken together, these data indicate that overexpressed MIR1, when not released from microtubules, interferes with mitosis and spindle morphology.

Analysis of microtubule binding

How does the phosphorylation of the P-stretch affect the microtubule-binding properties of MIR1? One could imagine that the P-stretch itself binds to microtubules in a phosphorylation-dependent manner or that phosphorylation of the P-stretch affects other domains important for microtubule binding. To test these possibilities, we made deletion mutants of MIR1. The truncations tN and tNP both contained the N-terminal domains, but tNP also contains a small region including the P-stretch (Fig. 6A). tPC and tC both contained the C-terminal B30.2 box and again only differ by the presence of the P-stretch in tPC. The N- and C-terminal constructs were expressed as cyan and yellow fluorescent fusion proteins (CFP and YFP), respectively. To our surprise, none of the constructs colocalized with the microtubule cytoskeleton and instead showed mostly diffuse staining (Fig. 9A). Fusion proteins containing only the region around the P-stretch or the Fn3- domain (tP and tFn3;

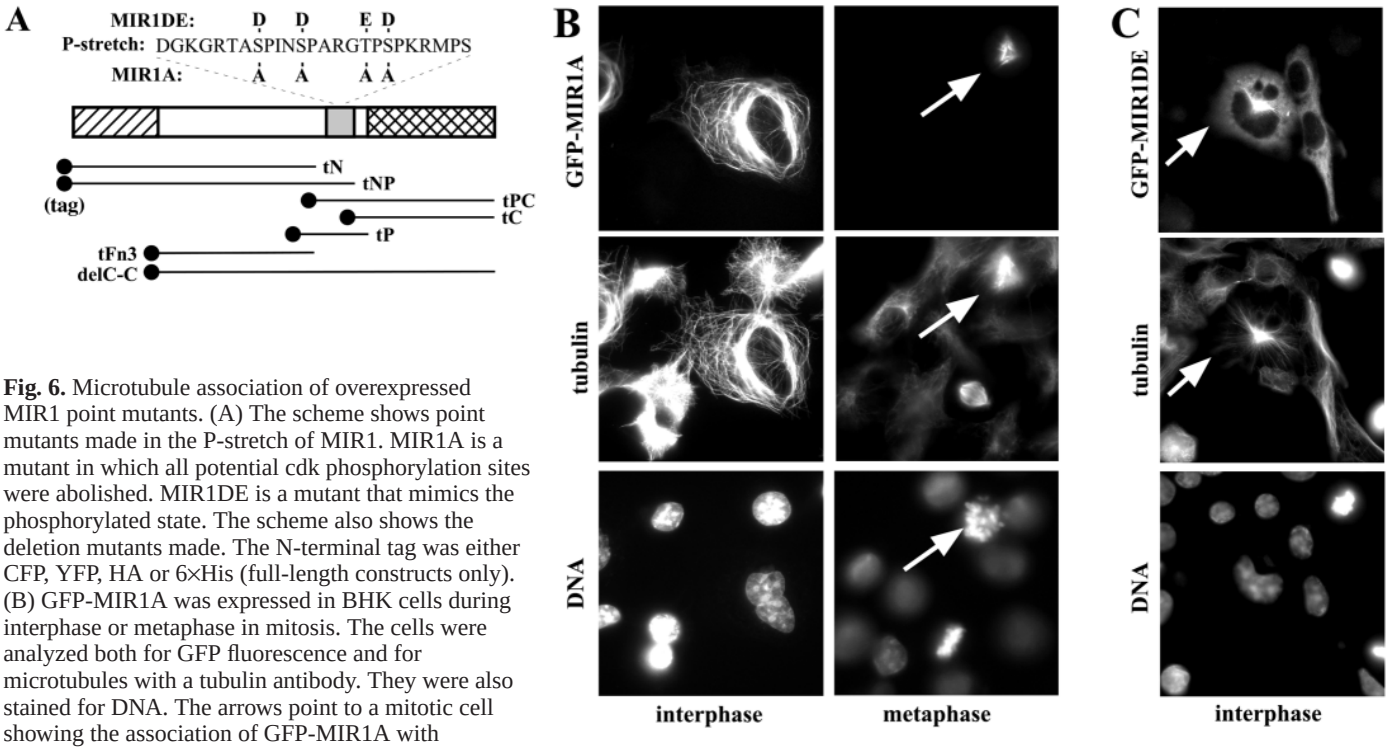

Fig. 6. Microtubule association of overexpressed MIR1 point mutants. (A) The scheme shows point mutants made in the P-stretch of MIR1. MIR1A is a mutant in which all potential cdk phosphorylation sites were abolished. MIR1DE is a mutant that mimics the phosphorylated state. The scheme also shows the deletion mutants made. The N-terminal tag was either CFP, YFP, HA or 6×His (full-length constructs only). (B) GFP-MIR1A was expressed in BHK cells during interphase or metaphase in mitosis. The cells were analyzed both for GFP fluorescence and for microtubules with a tubulin antibody. They were also stained for DNA. The arrows point to a mitotic cell showing the association of GFP-MIR1A with microtubules. (C) GFP-MIR1DE was expressed in interphase BHK cells. The cells were analyzed for GFP fluorescence and microtubule and DNA staining. The arrows point to a transfected cell showing the loss of association of GFP-MIR1DE with microtubules.

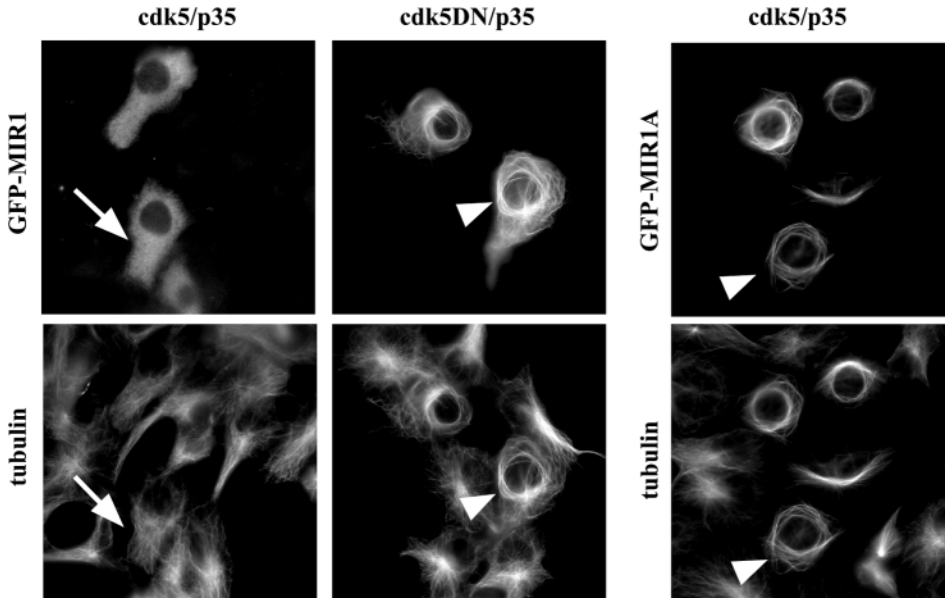

Fig. 7. Neuronal kinase cdk5 can modulate the affinity of MIR1 for microtubules. BHK cells were transfected with cdk5, its activator p35 and GFP-MIR1. Controls were performed with an inactive version of cdk5 (cdk5DN) and with GFP-MIR1A instead of the wild-type MIR1 fusion. Samples were processed for immunofluorescence microscopy 12 hours after transfection. The cells were analyzed for GFP fluorescence and for staining of microtubules. The arrow points to a cell expressing active cdk5 that shows diffuse MIR1 staining. The arrowheads point to cells expressing either inactive cdk5 or a non-phosphorylatable form of MIR1; these cells show colocalization of MIR1 and microtubules.

Fig. 6A) gave similar results (data not shown). At higher expression levels, both tPC and tC showed some concentration at the centrosome. At the highest expression levels, all constructs were prone to aggregation (data not shown).

Since none of the constructs showed significant association with microtubules in cells, we tested whether several MIR1 domains together could increase the interaction. N- and C-terminal constructs were cotransfected into BHK cells, and the localization of both fragments was detected simultaneously by CFP and YFP fluorescence. Three combinations of constructs showed only diffuse staining, but the combination of tNP with tPC directed both fragments to microtubules and induced the whorl phenotype seen with the intact wild-type protein (Fig. 9B). These results suggest that the N- and C-terminal fragments must associate with one another, mediated by overlapping P-stretches, to generate high microtubule affinity, and that MIR1 may function as a dimer or as an oligomer.

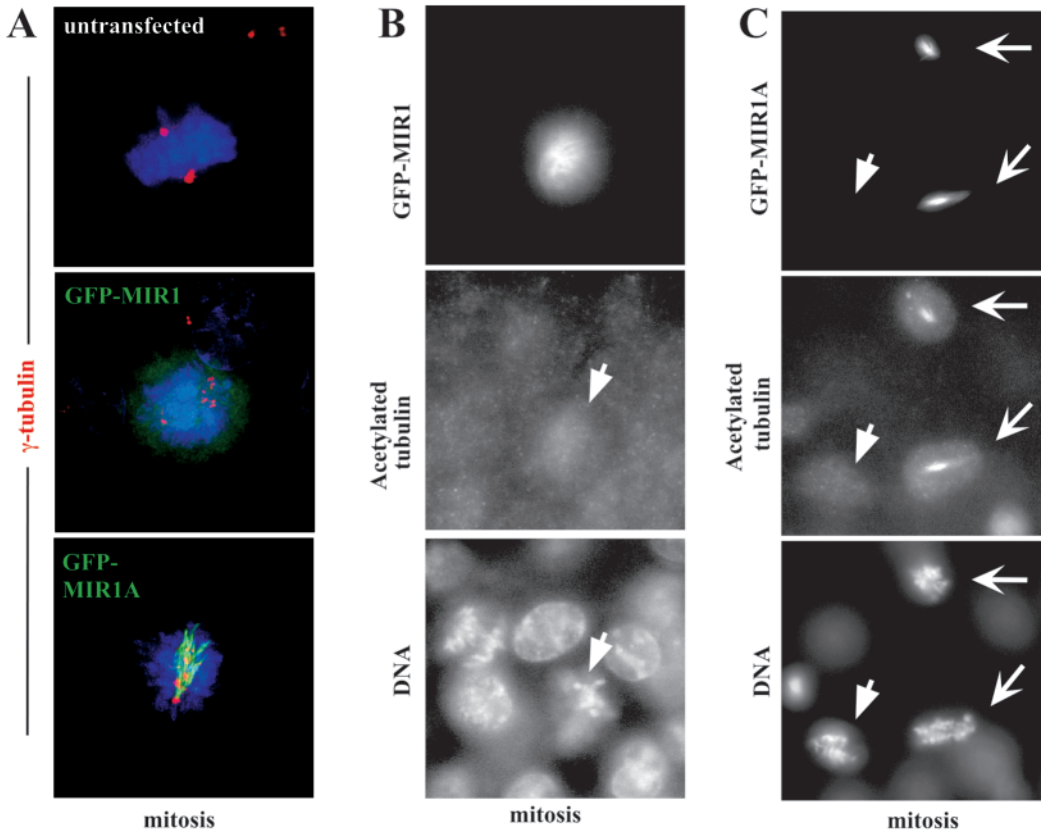

Fig. 8. Effect of overexpression of MIR1 on mitotic spindles. (A) Mitotic BHK cells expressing GFP-MIR1 (middle panel) or GFP-MIR1A (bottom panel) were analyzed for GFP fluorescence (green) and stained for γ-tubulin with mAb GTU-88 (red) and for DNA with Hoechst dye 33258 (blue). Images were acquired with a Deltavision system and processed as in Fig. 2C. (B) Mitotic BHK cells expressing GFP-MIR1 were analyzed for GFP fluorescence and for stable microtubules using an antibody 6-11B-1 against acetylated tubulin. (C) As in B, but with cells expressing GFP-MIR1A. The arrows point to a transfected cell, the arrowhead to an untransfected cell.

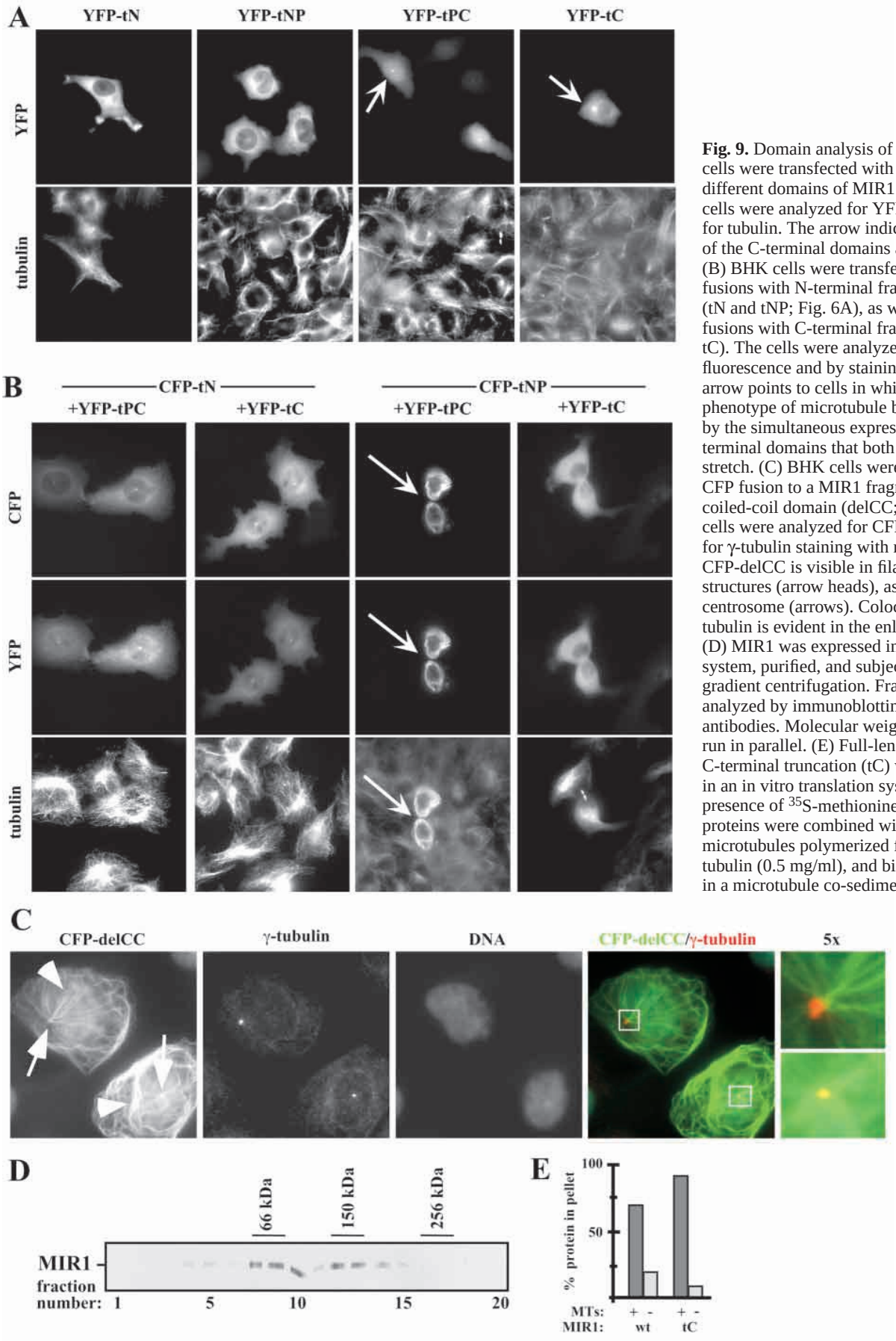

Fig. 9. Domain analysis of MIR1. (A) BHK cells were transfected with YFP fusions with different domains of MIR1 (Fig. 6A). The cells were analyzed for YFP fluorescence and for tubulin. The arrow indicates concentration of the C-terminal domains at the centrosome. (B) BHK cells were transfected with CFP fusions with N-terminal fragments of MIR1 (tN and tNP; Fig. 6A), as well as with YFP fusions with C-terminal fragments (tPC and tC). The cells were analyzed by CFP and YFP fluorescence and by staining for tubulin. The arrow points to cells in which the wild-type phenotype of microtubule bundling is restored by the simultaneous expression of N- and C-terminal domains that both contain the P-stretch. (C) BHK cells were transfected with a CFP fusion to a MIR1 fragment lacking the coiled-coil domain (delCC; Fig. 6A). The cells were analyzed for CFP fluorescence and for γ-tubulin staining with mAb GTU-88. CFP-delCC is visible in filaments and bundled structures (arrow heads), as well as at the centrosome (arrows). Colocolization with γ-tubulin is evident in the enlarged field. (D) MIR1 was expressed in a baculovirus system, purified, and subjected to sucrose gradient centrifugation. Fractions were analyzed by immunoblotting with MIR1 antibodies. Molecular weight standards were run in parallel. (E) Full-length MIR1 (wt) or a C-terminal truncation (tC) were synthesized in an in vitro translation system in the presence of ^{35}S-methionine. The labeled proteins were combined with an excess of microtubules polymerized from purified tubulin (0.5 mg/ml), and binding was assessed in a microtubule co-sedimentation assay.

This notion is further supported by the behavior of a MIR1 construct that lacked only the N-terminal coiled-coil domain (delCC). In contrast to the behavior of the other truncations, a fusion of delCC fusion to CFP showed filamentous staining in BHK cells. When the fusion was highly expressed, the filaments were bundled (see Fig. 9C, first panel, arrow heads), whereas at low expression levels, a diffuse staining was seen, indicating that delCC has a lower affinity for microtubules than the wild-type protein does (data not shown). Thus, it appears that the N-terminal coiled-coil domain is not essential for the interaction of MIR1 with microtubules.

Interestingly, the fusion protein CFP-delCC not only localized along microtubules, but in approximately 20% of the transfected cells was also found as a concentrated spot (Fig. 9C, first panel arrow). This spot corresponded to the location of the centrosome, as demonstrated by colocalization with γ-tubulin (Fig. 9C, second and last panel, plus the enlarged view). The occurrence of overexpressed delCC at the centrosome is in agreement with the localization of endogenous MIR1.

To examine further the assembly state of MIR1, we analyzed purified recombinant MIR1 protein using sucrose density gradients. Althoug the predicted molecular weight for MIR1 is around 60 kDa, the protein was found in fractions corresponding to a molecular weight of up to 150 kDa (Fig. 9D). This result suggests that MIR1 can form dimers or trimers. Oligomerization of MIR1 was also supported by co-immunoprecipitation experiments employing myc-tagged and GFP-tagged tN fragments co-expressed in BHK cells (data not shown). Taken together, these results suggest that MIR1 may self-associate to generate high affinity microtubule binding, possibly by generating multiple binding sites in the oligomeric assembly.

Finally, we sought to identify the microtubule-binding domain in MIR1. To test microtubule binding of the C-terminal domains, we used a microtubule-pelleting assay, which is more sensitive than localization in transfected cells. In vitro translated ^{35}S-methionine labelled GFP-MIR1 constructs were incubated in the absence or presence of taxol-stabilized microtubules polymerized from purified tubulin. The samples were spun briefly through a sucrose cushion to sediment microtubules, and the co-sedimentation of MIR1 protein was analyzed. Both the C-terminal fragment tCP and the full-length protein were highly enriched in the pellet fraction when microtubules were present (Fig. 9E). These results indicate that the B30.2 box contains a microtubule-binding site. The N-terminal fragment tNP was found in the pellet fraction even in the absence of microtubules and thus was not informative (data not shown).

Discussion

We have used a visual screen to identify a novel protein with microtubule-binding activity, called MIR1. We have shown microtubule association of overexpressed MIR1 by colocalization both in a steady-state situation and when new microtubules emerge from the centrosome, as well as by co-sedimentation. The specificity of microtubule association is also supported by experiments with a MIR1 point mutant that mimics the phosphorylated state of the protein during mitosis and has a lowered affinity for the polymer. In addition, our domain analysis also shows the specificity of the interaction, particularly the observation that overlapping fragments were required to obtain strong microtubule binding. Despite the fact that our data identify overexpressed MIR1 as a microtubule-binding protein, its function in vivo is less clear. Endogenous MIR1 was not found on microtubules but rather associated with the centrosome during interphase. Even the slightest overexpression of the full-length protein resulted in staining of microtubule filaments rather than the centrosome. Interestingly, however, an overexpressed MIR1 deletion construct was found both along microtubules and at the centrosome. In addition, an antibody to the full-length protein occasionally stained single microtubules. One possibility to reconcile these data is that MIR1 normally binds to a subclass of microtubules localized at the centrosome. When the full-length protein is overexpressed, its high affinity for the dense microtubule network and its tendency to self-associate may prevent localization to centrosomes. Centrosome binding of the endogenous protein may be controlled by a partner protein present at low concentrations. The postulated partner is probably a permanent component of the centrosome, rather than a motor protein that concentrates MIR1 at the site, because the endogenous localization of MIR1 is not affected by the disruption of microtubules. We do not believe that MIR1 binding is restricted to microtubules of the centriolar walls, because in most cell lines tested we observed staining that extended beyond the characteristic centriolar staining. We also observed some staining reminiscent of the Golgi, raising the possibility that MIR1 may be associated with a membraneous structure in the vicinity of centrosomes.

During the transition from interphase to mitosis, endogenous MIR1 is largely released from centrosomes. Our observation that overexpressed MIR1 is released from microtubules during mitosis suggests that endogenous MIR1 is released from a microtubule-containing structure at the centrosome. The decreased affinity of MIR1 for microtubule filaments could allow for increased dynamics of the filaments required during mitosis. Many characterized centrosomal proteins show a behavior opposite to MIR1: they are enriched in spindle poles during mitosis and increase the nucleation capacity of spindle poles (Mack et al., 2000; Urbani and Stearns, 1999; Zimmerman and Doxsey, 2000). However, there are a few centrosomal proteins that dissociate from centrosomes during mitosis. One of them, C-Nap, dissociates as the replicated centrosomes separate and is believed to be involved in cohesion of the centrosomes (Fry et al., 1998; Mayor et al., 2000). By contrast, MIR1 continues to reside on separated centrosomes and is therefore unlikely to be involved in cohesion.

MIR1 dissociates from centrosomes at the G2 to M transition, which is coincident with cdk1 activation, and reappears on spindle poles in late anaphase, when cdk1 is inactivated. Overexpressed MIR1 dissociates from microtubules with the same time course. When the predicted cdk-phosphorylation sites in a P-stretch are abolished, the affinity of MIR1 for microtubules is maintained during mitosis; conversely, mutations in the P-stretch that mimic the phosphorylated state decrease the affinity of MIR1 for microtubules. Phosphorylation in the P-stretch by cdk5 also reduces microtubule binding. Our data therefore suggest that MIR1 dissociates from centrosomes upon phosphorylation in the P-stretch by a cyclin-dependent kinase.

Although overexpressed wild-type MIR1 is largely

dissociated from microtubules during mitosis, it still affects spindle poles: γ-tubulin is often splayed out rather than concentrated at the spindle poles. This phenotype is reminiscent of effects resulting from the suppression of dynein/dynactin activity, which have been interpreted as a lack of spindle pole cohesion (Echeverri et al., 1996; Heald et al., 1996). It is possible that a component involved in keeping a spindle pole together is sequestered by MIR1 overexpression.

Previous studies on MID1/midin and MID2 and our deletion analysis show that the major microtubule-binding site seems to be in the C-terminal B30.2 box. However, this domain alone interacts only weakly with microtubules. A stronger association with microtubules is observed with MIR1 constructs that contain both the Fn3 domain and the B30.2 box. We believe that the full-length protein has an increased microtubule affinity because it can oligomerize more effectively, thereby allowing microtubule binding of multiple domains. Oligomerization of MIR1 is supported by a number of observations: dimers or trimers of purified MIR1 are observed in sucrose gradient centrifugation, differently tagged MIR1 molecules can be co-immunoprecipitated and N- and C-terminal fragments expressed together can bind strongly to microtubules only if each of them contains the P-stretch. Finally, when MIR1 is expressed at low levels in cells, it is found along a few microtubule filaments rather than distributed evenly on microtubules throughout the cell, suggesting that there is cooperative binding. Phosphorylation of the P-stretch could decrease the affinity for microtubules by disrupting the oligomerization of MIR1 or it could cause a conformational change in the oligomer.

Although our data indicate that MIR1 is a novel centrosome-associated protein, its function remains to be clarified. The centrosome is engaged in many different activities that may even be cell-type specific. MIR1 is prominently expressed in only a subset of tissues, particularly in the adult brain, and it therefore is likely to play a more specialized role in the centrosome or in microtubule dynamics.

We are grateful to Ken Kosik, Tim Mitchison, Puck Ohi and David Pellman for insightful discussions, and to Tim Mitchison, David Pellman and Will Prinz for critiquing the manuscript. Rani Dhavan and Maria Morabito in the laboratory of Li-Huei Tsai supplied the cdk5 reagents. We thank the members of the Rapoport laboratory for contributions large and small. T.A.R. is a Howard Hughes Medical Institute investigator.

References

Andersen, S. S. (1998). *Xenopus* interphase and mitotic microtubule-associated proteins differentially suppress microtubule dynamics in vitro. *Cell Motil. Cytoskeleton* **41**, 202-213.

Belmont, L. D. and Mitchison, T. J. (1996). Identification of a protein that interacts with tubulin dimers and increases the catastrophe rate of microtubules. *Cell* **84**, 623-631.

Bobinnec, Y., Khodjakov, A., Mir, L. M., Rieder, C. L., Edde, B. and Bornens, M. (1998). Centriole disassembly in vivo and its effect on centrosome structure and function in vertebrate cells. *J. Cell Biol.* **143**, 1575-1589.

Borisy, G. G., Marcum, J. M., Olmsted, J. B., Murphy, D. B. and Johnson, K. A. (1975). Purification of tubulin and associated high molecular weight proteins from porcine brain and characterization of microtubule assembly in vitro. *Ann. NY Acad. Sci.* **253**, 107-132.

Buchner, G., Montini, E., Andolfi, G., Quaderi, N., Cainarca, S., Messali, S., Bassi, M. T., Ballabio, A., Meroni, G. and Franco, B. (1999). MID2, a homologue of the Opitz syndrome gene MID1: similarities in subcellular localization and differences in expression during development. *Hum. Mol. Genet.* **8**, 1397-1407.

Bulinski, J. C. and Borisy, G. G. (1980). Widespread distribution of a 210,000 mol wt microtubule-associated protein in cells and tissues of primates. *J. Cell Biol.* **87**, 802-808.

Bulinski, J. C., Richards, J. E. and Piperno, G. (1988). Posttranslational modifications of alpha tubulin: detyrosination and acetylation differentiate populations of interphase microtubules in cultured cells. *J. Cell Biol.* **106**, 1213-1220.

Cainarca, S., Messali, S., Ballabio, A. and Meroni, G. (1999). Functional characterization of the Opitz syndrome gene product (midin): evidence for homodimerization and association with microtubules throughout the cell cycle. *Hum. Mol. Genet.* **8**, 1387-1396.

Cox, T. C., Allen, L. R., Cox, L. L., Hopwood, B., Goodwin, B., Haan, E. and Suthers, G. K. (2000). New mutations in MID1 provide support for loss of function as the cause of X-linked Opitz syndrome. *Hum. Mol. Genet.* **9**, 2553-2562.

Desai, A. and Mitchison, T. J. (1997). Microtubule polymerization dynamics. *Annu. Rev. Cell Dev. Biol.* **13**, 83-117.

Dictenberg, J. B., Zimmerman, W., Sparks, C. A., Young, A., Vidair, C., Zheng, Y., Carrington, W., Fay, F. S. and Doxsey, S. J. (1998). Pericentrin and gamma-tubulin form a protein complex and are organized into a novel lattice at the centrosome. *J. Cell Biol.* **141**, 163-174.

Echeverri, C. J., Paschal, B. M., Vaughan, K. T. and Vallee, R. B. (1996). Molecular characterization of the 50-kD subunit of dynactin reveals function for the complex in chromosome alignment and spindle organization during mitosis. *J. Cell Biol.* **132**, 617-633.

Fry, A. M., Mayor, T., Meraldi, P., Stierhof, Y. D., Tanaka, K. and Nigg, E. A. (1998). C-Nap1, a novel centrosomal coiled-coil protein and candidate substrate of the cell cycle-regulated protein kinase Nek2. *J. Cell Biol.* **141**, 1563-1574.

Hartman, J. J., Mahr, J., McNally, K., Okawa, K., Iwamatsu, A., Thomas, S., Cheesman, S., Heuser, J., Vale, R. D. and McNally, F. J. (1998). Katanin, a microtubule-severing protein, is a novel AAA ATPase that targets to the centrosome using a WD40-containing subunit. *Cell* **93**, 277-287.

Heald, R., Tournebize, R., Blank, T., Sandaltzopoulos, R., Becker, P., Hyman, A. and Karsenti, E. (1996). Self-organization of microtubules into bipolar spindles around artificial chromosomes in *Xenopus* egg extracts. *Nature* **382**, 420-425.

Hellmich, M. R., Pant, H. C., Wada, E. and Battey, J. F. (1992). Neuronal cdc2-like kinase: a cdc2-related protein kinase with predominantly neuronal expression. *Proc. Natl. Acad. Sci. USA* **89**, 10867-10871.

Henry, J., Mather, I. H., McDermott, M. F. and Pontarotti, P. (1998). B30.2-like domain proteins: update and new insights into a rapidly expanding family of proteins. *Mol. Biol. Evol.* **15**, 1696-1705.

Hyman, A. A. and Karsenti, E. (1996). Morphogenetic properties of microtubules and mitotic spindle assembly. *Cell* **84**, 401-410.

Kellogg, D. R., Field, C. M. and Alberts, B. M. (1989). Identification of microtubule-associated proteins in the centrosome, spindle, and kinetochore of the early *Drosophila* embryo. *J. Cell Biol.* **109**, 2977-2991.

Lewis, S. A., Ivanov, I. E., Lee, G. H. and Cowan, N. J. (1989). Organization of microtubules in dendrites and axons is determined by a short hydrophobic zipper in microtubule-associated proteins MAP2 and tau. *Nature* **342**, 498-505.

Lippincott-Schwartz, J. (1998). Cytoskeletal proteins and Golgi dynamics. *Curr. Opin. Cell Biol.* **10**, 52-59.

Mack, G. J., Ou, Y. and Rattner, J. B. (2000). Integrating centrosome structure with protein composition and function in animal cells. *Microsc. Res. Tech.* **49**, 409-419.

Mayor, T., Stierhof, Y. D., Tanaka, K., Fry, A. M. and Nigg, E. A. (2000). The centrosomal protein C-Nap1 is required for cell cycle-regulated centrosome cohesion. *J. Cell Biol.* **151**, 837-846.

Meyerson, M., Enders, G. H., Wu, C. L., Su, L. K., Gorka, C., Nelson, C., Harlow, E. and Tsai, L. H. (1992). A family of human cdc2-related protein kinases. *EMBO J.* **11**, 2909-2917.

Mogensen, M. M., Malik, A., Piel, M., Bouckson-Castaing, V. and Bornens, M. (2000). Microtubule minus-end anchorage at centrosomal and non-centrosomal sites: the role of ninein. *J. Cell Sci.* **113**, 3013-3023.

Nikolic, M., Dudek, H., Kwon, Y. T., Ramos, Y. F. and Tsai, L. H. (1996). The cdk5/p35 kinase is essential for neurite outgrowth during neuronal differentiation. *Genes Dev.* **10**, 816-825.

Perry, J., Short, K. M., Romer, J. T., Swift, S., Cox, T. C. and Ashworth, A. (1999). FXY2/MID2, a gene related to the X-linked Opitz syndrome gene FXY/MID1, maps to Xq22 and encodes a FNIII domain-containing protein that associates with microtubules. *Genomics* **62**, 385-394.

Quaderi, N. A., Schweiger, S., Gaudenz, K., Franco, B., Rugarli, E. I., Berger, W., Feldman, G. J., Volta, M., Andolfi, G., Gilgenkrantz, S. et al. (1997). Opitz G/BBB syndrome, a defect of midline development, is due to mutations in a new RING finger gene on Xp22. *Nat. Genet.* **17**, 285-291.

Quintyne, N. J., Gill, S. R., Eckley, D. M., Crego, C. L., Compton, D. A. and Schroer, T. A. (1999). Dynactin is required for microtubule anchoring at centrosomes. *J. Cell Biol.* **147**, 321-334.

Rolls, M. M., Stein, P. A., Taylor, S. S., Ha, E., McKeon, F. and Rapoport, T. A. (1999). A visual screen of a GFP-fusion library identifies a new type of nuclear envelope membrane protein. *J. Cell Biol.* **146**, 29-44.

Schulze, E., Asai, D. J., Bulinski, J. C. and Kirschner, M. (1987). Posttranslational modification and microtubule stability. *J. Cell Biol.* **105**, 2167-2177.

Schweiger, S., Foerster, J., Lehmann, T., Suckow, V., Muller, Y. A., Walter, G., Davies, T., Porter, H., van Bokhoven, H., Lunt, P. W. et al. (1999). The Opitz syndrome gene product, MID1, associates with microtubules. *Proc. Natl. Acad. Sci. USA* **96**, 2794-2799.

Shirasu, M., Yonetani, A. and Walczak, C. E. (1999). Microtubule dynamics in *Xenopus* egg extracts. *Microsc. Res. Tech.* **44**, 435-445.

Stearns, T. (2001). Centrosome duplication. a centriolar pas de deux. *Cell* **105**, 417-420.

Tsai, L. H., Takahashi, T., Caviness, V. S., Jr and Harlow, E. (1993). Activity and expression pattern of cyclin-dependent kinase 5 in the embryonic mouse nervous system. *Development* **119**, 1029-1040.

Tsai, L. H., Delalle, I., Caviness, V. S., Jr, Chae, T. and Harlow, E. (1994). p35 is a neural-specific regulatory subunit of cyclin-dependent kinase 5. *Nature* **371**, 419-423.

Urbani, L. and Stearns, T. (1999). The centrosome. *Curr. Biol.* **9**, R315-R317.

Westendorf, J. M., Rao, P. N. and Gerace, L. (1994). Cloning of cDNAs for M-phase phosphoproteins recognized by the MPM2 monoclonal antibody and determination of the phosphorylated epitope. *Proc. Natl. Acad. Sci. USA* **91**, 714-718.

Zheng, Y., Wong, M. L., Alberts, B. and Mitchison, T. (1995). Nucleation of microtubule assembly by a gamma-tubulin-containing ring complex. *Nature* **378**, 578-583.

Zimmerman, W. and Doxsey, S. J. (2000). Construction of centrosomes and spindle poles by molecular motor-driven assembly of protein particles. *Traffic* **1**, 927-934.